

# Genome-wide identification of CYP90 family and functional analysis of *NnCYP90B1* on rhizome enlargement in lotus

Minghua Zhang<sup>1,2,3</sup>, Heyun Song<sup>1,2,3</sup>, Xianbao Deng<sup>1,2</sup> and Mei Yang<sup>1,2\*</sup>

<sup>1</sup> Aquatic Plant Research Center, Wuhan Botanical Garden, Chinese Academy of Sciences, Wuhan 430074, China

<sup>2</sup> Hubei Key Laboratory of Wetland Evolution & Ecological Restoration, Wuhan Botanical Garden, Chinese Academy of Sciences, Wuhan 430074, China

<sup>3</sup> University of Chinese Academy of Sciences, 19A Yuquanlu, Beijing 100049, China

\* Corresponding author, E-mail: [yangmei815815@wbgcas.cn](mailto:yangmei815815@wbgcas.cn)

## Abstract

The CYP90 family is a crucial group of enzymes involved in the structural modification of brassinosteroids (BRs) and plays a pivotal role in regulating plant growth and development. However, information regarding the CYP90 family in lotus remains limited. Here, five members of the CYP90 family were identified in the lotus genome, distributed across four chromosomes. Analysis of exon/intron arrangements revealed that all *NnCYP90* genes contained eight exons. Furthermore, all *NnCYP90* proteins were found to be located within the endoplasmic reticulum and contained a typical heme-binding region. The promoter regions of *NnCYP90* harbor numerous *cis*-acting elements associated with responses to light signals, hormone signals, plant growth, and development, as well as abiotic and biotic stress. The members of the *NnCYP90* family were expressed in at least one tissue, with three genes in the *NnCYP90B* and *NnCYP90D* subfamilies exhibiting specific expression in underground tissues. *NnCYP90B1*, identified as a key rate-limiting enzyme in the BR synthesis pathway, displayed high expression levels in the rhizome of the temperate ecotype 'ZO', whereas its expression in the rhizome of the tropical ecotype 'DH' was comparatively low. Moreover, *NnCYP90B1* expression was higher in the rhizome at the swelling stage than at the stolon stage. Overexpression of *NnCYP90B1* in *Solanum tuberosum* resulted in early tuberization and increased tuber yield. Taken together, this study elucidates the genetic characteristics of the lotus CYP90 family genes and provides insights into the role of *NnCYP90B1* in lotus rhizome development. These findings shed new light on the mechanisms underlying lotus rhizome enlargement.

**Citation:** Zhang M, Song H, Deng X, Yang M. 2024. Genome-wide identification of CYP90 family and functional analysis of *NnCYP90B1* on rhizome enlargement in lotus. *Vegetable Research* 4: e035 <https://doi.org/10.48130/vegres-0024-0033>

## Introduction

Lotus (*Nelumbo nucifera* Gaertn.) is a perennial aquatic plant widely cultivated across Asian countries for its ornamental, edible, and medicinal values<sup>[1]</sup>. To thrive in the varied environments of Asia, the lotus has evolved into two ecological types, tropical and temperate, each adapting to different ecological habitats. Tropical lotus mainly grows in tropical regions like Hainan Province (China), Thailand, and South India. It grows continuously throughout the year without an obvious dormancy period. On the other hand, temperate lotus thrives in subtropical areas, such as central China, Japan, Iran, and north-central India. The temperate lotus follows distinct seasonal growth cycles, typically commencing germination in April, blooming from June to August, withering in early September, and entering dormancy from November to March of the subsequent year<sup>[2]</sup>.

The lotus rhizome is a storage organ derived from a modified subterranean stem. It acts as a reproductive organ for asexual production, which is a predominant method of propagation in lotus. The development of rhizome is a complex process that involves four main stages: stolon stage (elongating longitudinally), initial swelling (increasing in girth), middle swelling (continuing expansion with gradual starch accumulation), and later swelling stage (enlargement ceases and starch accumulates rapidly)<sup>[3]</sup>. Temperate lotus rhizomes progress all four developmental stages. Successful rhizome enlargement

ensures lotus survival through cold winters, allowing it to sprout in the upcoming spring season. In contrast, tropical lotus does not undergo significant enlargement throughout its entire growth period and cannot withstand the cold when cultivated in subtropical and temperate regions. Therefore, rhizome enlargement is an adaptive strategy for lotus to survive in cold weather<sup>[4,5]</sup>.

Rhizome enlargement is regulated by a combination of external environment stimuli and endogenous regulatory signaling. Similar to tuberous plants, low temperatures and short day length (SD) stimulate lotus rhizome enlargement, while high temperatures and long day length (LD) promote rhizome horizontal elongation<sup>[6,7]</sup>. In addition, hormones, as key endogenous signals in plants have been extensively reported to be involved in the initiation and growth of storage organs. In lotus, the transition of rhizome from longitudinal elongation to girth enlargement is also regulated through the biosynthesis of gibberellins (GA) and abscisic acid (ABA)<sup>[8,9]</sup>. However, the impact of other hormones on lotus rhizome enlargement remains unexplored.

Brassinosteroid (BR), a phytohormone identified in recent decades, plays a pivotal role in plant growth, cell division, elongation, and reproductive development<sup>[10,11]</sup>. Research confirmed that BR hormones regulate physiological and developmental processes in tuberous plants. Exogenous application of epibrassinolide (EBR) has notably enhanced tuber enlargement

in *Pinellia ternata*, *Solanum tuberosum*, and *Allium cepa*<sup>[12–15]</sup>. Key biosynthetic enzymes of the BR signaling pathway, including DWF4, CPD, DET2, and ROT3/CYP90D1, are classified as the CYP90 family<sup>[16,17]</sup>. These enzymes, identified primarily through the generation of corresponding plant mutants, are highly conserved. Several BR-deficient *Arabidopsis* mutants, such as *constitutive photomorphogenesis* and *dwarfism (cpd)*, *dwarf4 (dwf4)*, and *rotundifolia3 (rot3)*, are attributed to *AtCYP90A1*, *AtCYP90B1*, and *AtCYP90C1* defects, respectively<sup>[18–20]</sup>. In rice, BR biosynthesis mutants such as *ebisu dwarf (d2)* and *osdwarf4-1* carry mutations in *OsCYP90D2* and *OsCYP90B*, respectively<sup>[21]</sup>. The tomato mutant *dwarf* is defective in *CYP85A*, and the *dumpy* mutation affects an ortholog of *AtCYP90A1*<sup>[22,23]</sup>.

To date, *CYP90* genes in lotus have not been identified, leaving their role in lotus growth and development yet to be revealed. Recently, a major quantitative trait locus (QTL) for rhizome enlargement in lotus was pinpointed, termed cqREI-LG2, and successfully validated the function of a candidate gene, *NnBEL6*, within this interval in promoting rhizome enlargement<sup>[5]</sup>. Intriguingly, *Nn5g29581*, a gene belonging to the *CYP90B* subfamily, is flanked to the cqREI-LG2 locus. To investigate its role in promoting rhizome enlargement, members of the *CYP90* family in lotus were first identified, and subsequently a comprehensive analysis was conducted of their evolution, gene structures, and expression patterns. Additionally, its function on plant tuber development was assessed by heterologously overexpressing *Nn5g29581* in potato. These findings provide a basis for deeper insights into the mechanism underlying lotus rhizome enlargement.

## Materials and methods

### Plant materials and generation of transgenic plants

Temperate lotus 'ZhouOu (ZO)' and tropical lotus 'DongHonghua (DH)' were used in this study. Both varieties were cultivated under consistent management of water and fertilizer in an outdoor breeding base at the Wuhan Botanical Garden, Chinese Academy of Sciences (Wuhan, Hubei Province, China). Rhizomes of the two cultivars were separately planted on April 15, 2023. Samples for Real-Time quantitative PCR (RT-qPCR) were collected at 91 d (stolon stage) and 153 d (swelling stage) after planting, respectively. All samples were rapidly frozen in liquid nitrogen and stored at  $-80^{\circ}\text{C}$  until further use.

*Nicotiana benthamiana* was employed in a transient expression system. Seeds were germinated and grown in soil for two weeks before being transplanted into individual pots. These plants were maintained at a temperature of  $25 \pm 1^{\circ}\text{C}$  under a photoperiod of 16 h light and 8 h dark (LDs). *Solanum tuberosum* (E-Potato3, E3) served as stable heterologous transgenic material. Plants were grown in sterile culture bottles (12 cm  $\times$  8 cm) containing 50 mL of MS medium (pH 6.1) supplemented with 0.8% (w/v) agar. The growth chamber was maintained at  $25 \pm 1^{\circ}\text{C}$  under a light/dark cycle of LDs or 8 h light and 16 h dark (SDs).

### Identification of NnCYP90s and analysis of basic physicochemical properties

Access to lotus genome data was available through the National Genomics Data Center (<https://ngdc.cncb.ac.cn/gwh>). Candidate *NnCYP90* family members were extracted based on

gene annotations. Gene structural domains were predicted online using the NCBI website ([www.ncbi.nlm.nih.gov/Structure/cdd/wrpsb.cgi](http://www.ncbi.nlm.nih.gov/Structure/cdd/wrpsb.cgi)), and sequences with incomplete conserved structural domains were excluded. Predictions for protein isoelectric points were conducted using the ExPasy website (<https://web.expasy.org>). Protein instability coefficient and hydrophilicity predictions were performed using TBtools software<sup>[24]</sup>. Subcellular localization prediction was performed using Cell-PLoc 2.0 online software ([www.csbio.sjtu.edu.cn/bioinf/Cell-PLoc-2](http://www.csbio.sjtu.edu.cn/bioinf/Cell-PLoc-2))<sup>[25]</sup>.

### Bioinformatics analysis of NnCYP90s

The protein sequences belonging to the reported *CYP90* family from various species were downloaded from the NCBI website ([www.ncbi.nlm.nih.gov/protein](http://www.ncbi.nlm.nih.gov/protein)). Subsequently, the phylogenetic tree of *NnCYP90* was constructed using the neighbor-joining method with 1,000 bootstrap replications using MEGA 11.0. Conserved and functional motifs were analyzed using the MEME website (<https://meme-suite.org>), and gene structure and conserved protein motifs were visualized using TBtools. Clustal Omega ([www.ebi.ac.uk/Tools/msa/clustalo](http://www.ebi.ac.uk/Tools/msa/clustalo)) was used for multiple sequence alignments with the default parameters. Furthermore, *cis*-acting elements within the promoter regions of *NnCYP90* genes were explored by analyzing approximately 2,000 bp of sequence upstream of the translation initiation site were analyzed using PlantCARE (<http://bioinformatics.psb.ugent.be/webtools/plantcare/html>).

### Analyzing the expression patterns of the NnCYP90 genes

To investigate the expression profiles of the *NnCYP90* family genes in lotus tissues, transcriptome data corresponding to gene expression abundance was obtained from the RNA-seq raw data. The available RNA-seq raw data include various lotus tissues, leaves treated with methyl jasmonate (MeJA), and different embryo development periods<sup>[26–28]</sup>. Quality control of the downloaded transcriptome data sets were conducted using FastQC and Trimmomatic programs. Gene expression levels were quantified by Fragments Per Kilobase of transcript per Million mapped fragments (FPKM) using StringTie software. Subsequently, gene expression profiles were visualized using TBtools software.

### Subcellular localization assay

The coding region of *NnCYP90B1* was cloned into the vector (pMDC83) with primers (Table 1) using ClonExpress II One Step Cloning Kit, following the manufacturer's protocol (C112-01, Vazyme, Nanjing, China). Positive plasmids were extracted from *Escherichia coli* TOP10, as determined by colony PCR, and subsequently transformed into *Agrobacterium tumefaciens* GV3101 via electroporation. An additional *Agro* strain carrying an ER-marker was included as an endoplasmic reticulum location indicator. Suspensions containing ER-marker *Agro* and suspensions containing pMDC83 constructs *Agro* were mixed in equal volumes, resulting in a concentration of  $\text{OD}_{600} = 0.3$  for each *Agro* strain. The mixed suspension was then incubated at room temperature for 2–3 h and subsequently infiltrated into 4–5-week-old tobacco leaves using a needleless 1 mL syringe. The plants were kept in the dark for 24 h and then transferred to LD conditions. After 3 d, the fluorescence signals of GFP and RFP on the abaxial side of tobacco leaves were observed using a confocal laser scanning microscope (Leica TCS SP8, Leica Microsystems CMS GmbH, Germany).

**Table 1.** Primer sequences.

| Gene name            | Forward primer (5'-3') | Reverse primer (5'-3') |
|----------------------|------------------------|------------------------|
| <i>qRT-NnActin</i>   | CTCCGTGTTGCCCTGAAG     | CCAGCAAGGTCCAACCGAAG   |
| <i>qRT-NnCYP90B1</i> | TTCCTCGGGTGGGATTGA     | CTTGTTCTTGGCTCGGGCA    |
| <i>qRT-StActin</i>   | GGAAAAGCTTGCCATATGTTGG | CTGCTCCTGGCAGTTTCAA    |
| <i>qRT-StSP6A</i>    | GACGATCTCGCAACTTTTACA  | CCTCAAGTTAGGGTCGCTTG   |
| <i>qRT-StSP5G</i>    | CTTTGGCAATGAAGTCGTGGG  | GCAGCCAATTGTCGATACAAC  |
| <i>NnCYP90B1</i>     | ATGGCTGCTGAAATAGAGCTT  | ACATGGGAGGCTGAGAGAGTTG |

### Real-Time quantitative PCR analysis

The expression of *NnCYP90B1* in various tissues and at two different rhizome development stages of 'ZO' and 'DH' was analyzed using RT-qPCR. Samples frozen in liquid nitrogen were ground into a fine powder, and total RNA was extracted using the Total RNApure Kit (ZOMANBIO, Beijing, China) following the manufacturer's instructions. The quality and quantity of RNA was assessed using NanoDrop (ND-LITE, Thermo Fisher, USA). First-strand cDNA was synthesized using the TransScript® II One-Step gDNA Removal and cDNA Synthesis SuperMix (TransGen, Beijing, China). RT-qPCR was performed using SYBR® Premix Ex Taq™ II (Takara, Dalian, China) on a StepOne-Plus™ Real-Time PCR system (Applied Biosystems, Foster City, CA, USA). *NnActin* (*Nn1g06108*) was used as an internal reference. Relative expression levels were calculated using the  $2^{-\Delta\Delta CT}$  method and all gene expression analyses were conducted with three biological replicates (n = 3). The primer sequences are listed in Table 1.

### Potato transformation

The GV3101 strain containing *35S::NnCYP90B1-GFP* was introduced into the stems of *S. tuberosum* lines, E3, following the transgenic methods outlined by Zhou et al.<sup>[29]</sup>. Briefly, the infected potato stem segments were co-cultivated on MS medium and kept in the dark for 3 d. Then the stem segments were washed with sterile water and transferred to a callus induction medium (CIM) under LDs conditions. The selected callus was then grown cultured on shoot induction medium (SIM). After bud differentiation, the buds were transferred to a rooting medium (RIM) to facilitate plant growth. Positive plants were identified through PCR using specific primers (Table 1). Two positive lines of transgenic potatoes were selected for an *in vitro* tuberization test.

For the tuberization test, approximately 2 cm of the shoot apex from the positive plants was excised and transplanted onto tuber induction medium under SD conditions. The MS medium was supplemented with 50 mg/L Kan, 1.2 g/L activated carbon, and 8% (w/v) sucrose. Tuber harvest occurred approximately three months later. The number and weight of the tubers were recorded. Furthermore, the expression levels of *NnCYP90B1* and the tuberization related genes, *StSP6A* and *StSP5G*, was detected by RT-qPCR<sup>[30]</sup>. Relative expression levels

were calculated using the  $2^{-\Delta CT}$  method, and all gene expression analyses were conducted with three biological replicates (n = 3) for each genotype. The potato actin gene (GenBank accession number: XM006350963) served as an internal control.

## Results

### Identification and chromosomal localizations of the *NnCYP90* family

Based on the gene annotation database of the reference genome<sup>[26]</sup>, five *NnCYP90* genes were identified in the lotus genome, and distributed across four of the eight lotus chromosomes. Specifically, *Nn2g11471* and *Nn2g13694* were located on Chromosome 2, while the remaining three genes, *Nn1g05015*, *Nn5g29581*, and *Nn6g35462*, were situated on Chromosomes 1, 5, and 6, respectively. The open reading frames of *NnCYP90* members ranged from 1,461 to 1,560 bp, with *Nn2g11471* encoding the shortest amino acid sequence and *Nn5g29581* the longest (Table 2). The theoretical isoelectric points (pI) and instability coefficients of *NnCYP90*s ranged from 8.04 to 9.48 and 43.69 to 56.69, respectively, indicating that all *CYP90* proteins of *N. nucifera* are basic and labile (instability coefficient > 40). Furthermore, the gravy values of all five lotus *CYP90* proteins were below zero, indicating their hydrophilic nature. Subcellular localization predictions suggested that all *NnCYP90*s are localized in the endoplasmic reticulum (ER), consistent with the localization properties of *CYP450*. Syntenic analysis between the *N. nucifera* and *N. lutea* genomes identified four *CYP90* orthologous gene pairs. Both *Nn1g05015* and *Nn5g29581* corresponded to *Al02631* on *N. lutea*, while *Nn2g11471*, *Nn2g13694*, *Nn6g35462* matched *Al19495*, *Al32099*, and *Al25018*, respectively.

### Phylogenetic analysis, gene structure, and conserved motifs of the *NnCYP90* family

To elucidate the evolutionary relationships of the lotus *CYP90*s, a phylogenetic tree was constructed using the reported *CYP90* genes from six species, including five dicots (*Arabidopsis thaliana*, *Glycine max*, *Theobroma cacao*, *Solanum lycopersicum*, and *Vitis vinifera*) and one monocot (*Oryza sativa*) (Fig. 1a). Generally, plant *CYP90*s were categorized into four clades (A–D). The five *NnCYP90*s were clustered in clade A (*Nn2g13694* and *Nn2g11471*), B (*Nn1g05015* and *Nn5g29581*), and D (*Nn6g35462*), respectively. Specifically, *Nn2g13694* is closely related to *OsCYP90A3* and *OsCYP90A4*, both of which play crucial roles as C23 $\alpha$ -hydroxylases in regulating BR biosynthesis and maintaining plant architecture in rice<sup>[31]</sup>. This suggests that *Nn2g13694* may also function as a *CYP90A*, which is involved in the BR synthesis and leaf development in lotus. Meanwhile, *Nn2g11471* showed high homology with *GmCYP90A1*, which is associated with flowering in soybean<sup>[32]</sup>. Notably, both *Nn1g05015* and *Nn5g29581* were clustered

**Table 2.** Information of *NnCYP90* family genes in the *Nelumbo nucifera* genome.

| Gene ID          | Start and end position (bp) | CDS (bp) | ORF (aa) | pI   | Instability coefficient | Gravy  | Subcellular localization | <i>N. lutea</i> homologous gene |
|------------------|-----------------------------|----------|----------|------|-------------------------|--------|--------------------------|---------------------------------|
| <i>Nn1g05015</i> | 103,609,705–103,613,149     | 1,500    | 499      | 8.04 | 43.69                   | −0.098 | Endoplasmic reticulum    | <i>Al02631</i>                  |
| <i>Nn2g11471</i> | 18,697,198–18,700,178       | 1,461    | 486      | 9.48 | 44.04                   | −0.093 | Endoplasmic reticulum    | <i>Al19495</i>                  |
| <i>Nn2g13694</i> | 54,396,989–54,400,435       | 1,476    | 491      | 8.60 | 45.26                   | −0.185 | Endoplasmic reticulum    | <i>Al32099</i>                  |
| <i>Nn5g29581</i> | 63,421,205–63,424,831       | 1,560    | 519      | 8.97 | 53.05                   | −0.215 | Endoplasmic reticulum    | <i>Al02631</i>                  |
| <i>Nn6g35462</i> | 64,896,537–64,902,600       | 1,554    | 517      | 9.39 | 56.69                   | −0.326 | Endoplasmic reticulum    | <i>Al25018</i>                  |

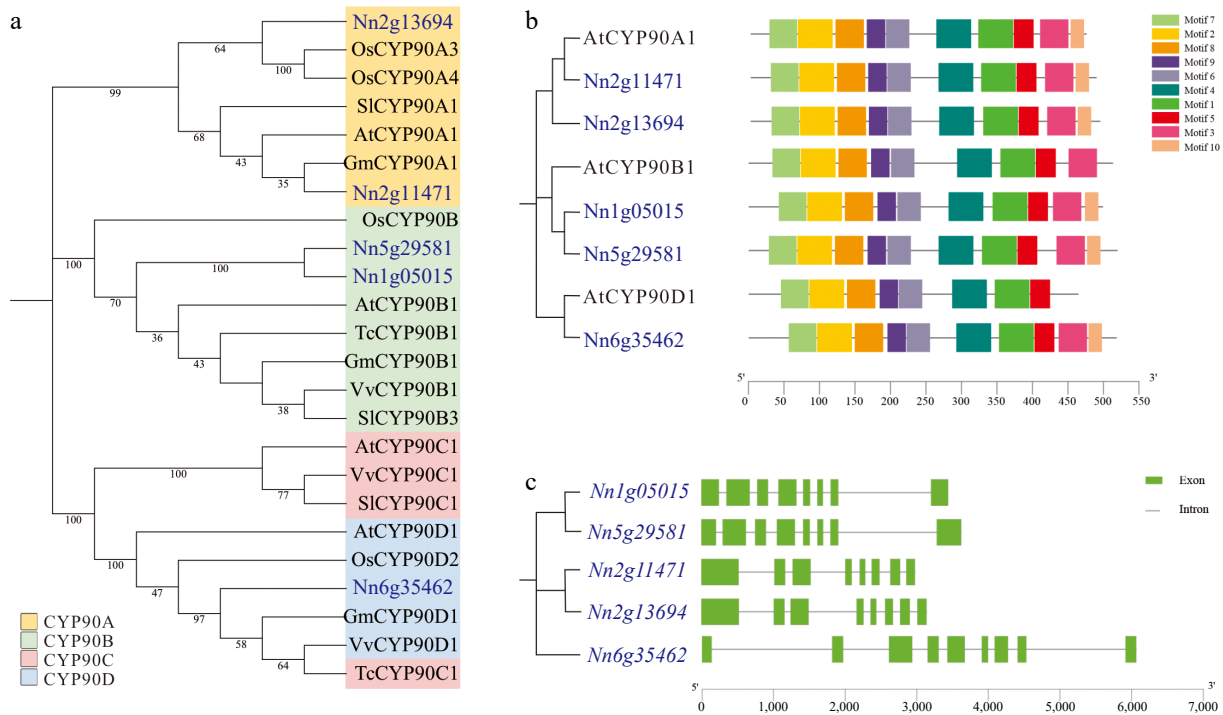


**Fig. 1** Phylogenetic analysis, conserved protein domains, and gene structures of NnCYP90 family. (a) Phylogenetic tree of the CYP90 protein family from *Nelumbo nucifera* (Nn), *Arabidopsis thaliana* (At), *Glycine max* (Gm), *Theobroma cacao* (Tc), *Solanum lycopersicum* (Sl), *Vitis vinifera* (Vv) and *Oryza sativa* (Os). The CYP90A, B, C, and D subfamilies are represented by yellow, green, red, and blue area, respectively. (b) Conserved domains analysis of CYP90 members in lotus and *Arabidopsis*. (c) Gene structures of NnCYP90 members.

closely with other CYP90Bs, presumed to be key rate-limiting enzymes in the BRs biosynthetic pathway, catalyzing the C22 $\alpha$ -hydroxylation reaction of the sterol skeleton<sup>[33]</sup>. This suggests that Nn1g05015 and Nn5g29581 likely function as hydroxylases, contributing to BR synthesis in lotus. In contrast, Nn6g35462 is located in the CYP90D clade, a subfamily that is also associated with BR synthesis. OsCYP90D2 catalyzed the steps from 6-deoxoteasterone to 3-dehydro-6-deoxoteasterone and from teasterone to 3-dehydroteasterone in the late BR biosynthesis pathway<sup>[21]</sup>. Notably, there is no NnCYP90 in the CYP90C clade in the lotus (Fig. 1a).

Assessment of conserved domains revealed conserved motifs in lotus CYP90s and their corresponding *Arabidopsis* CYP90s. All five NnCYP90s contained ten conserved motifs. Meanwhile, these conserved motifs were relatively evenly distributed between the N-terminal and C-terminal positions, with a slight difference in the degree of dispersion among members. In contrast, only AtCYP90A1 contained a complete set of ten conserved motifs, whereas AtCYP90B1 and AtCYP90D1 contained nine and eight, respectively (Fig. 1b). In addition, the gene structure of NnCYP90 was investigated. All five NnCYP90 genes contained eight exons, with genes within the same clade displaying similar intron and exon positions (Fig. 1c). Taken together, the results showed that all five lotus CYP90s contain similar conserved motifs and gene structures. The five lotus CYP90s can be classified into three different CYP90 subfamilies, suggesting lotus CYP90s probably are key enzymes involved in BR synthesis.

Amino acid sequence alignment of NnCYP90s, AtCYP90s, and OsCYP90s revealed highly conserved motifs in the NnCYP90s (Fig. 1b; Fig. 2). All NnCYP90s possess the conserved domains typical of CYP450s, including the heme-binding region

(FxxGxxxCxG), the PER domain with the characteristic signature (PWRW), and the ExxR motif in the K-helix region. Notably, the cysteine residues (Cys) within the heme-binding domain are essential for heme binding in CYP proteins. The result showed that this specific amino acid was completely conserved across all five NnCYP90s. In addition, the K-helix and PER domains play key roles in stabilizing the CYP fundamental structure by locking the heme pocket in its position. The ETLR sequence in the helix K region and the PWRW sequence in the PER domain were found to be identical across these CYP90 proteins, indicating the conservation of specific amino acid patterns characteristic of the CYP90 family. Additionally, the oxygen-binding domain (A/G)Gx(D/E)T(T/S) in the helix I region was commonly present in CYP90 family members, except for CYP90D.

### Analysis of *cis*-acting elements in the NnCYP90 gene promoters

*Cis*-acting elements within the promoter region play a pivotal role as molecular regulators, dictating the specific transcriptional activity and responsiveness of individual genes<sup>[34]</sup>. Here, *cis*-acting elements within the promoter regions of five NnCYP90 genes were analyzed. The investigation revealed a diverse array of *cis*-elements within the NnCYP90 promoter regions, encompassing numerous elements responsive to light, hormones, and stress, as well as elements associated with plant growth and development, alongside the foundational *cis*-acting elements, the TATA box and CAAT box (Fig. 3). Notably, elements related to abiotic stress, specifically LTR involved in low-temperature responsiveness were exclusively identified within the promoter regions of Nn2g13694 and Nn2g11471, both members of the CYP90A clade. Conversely, the promoters

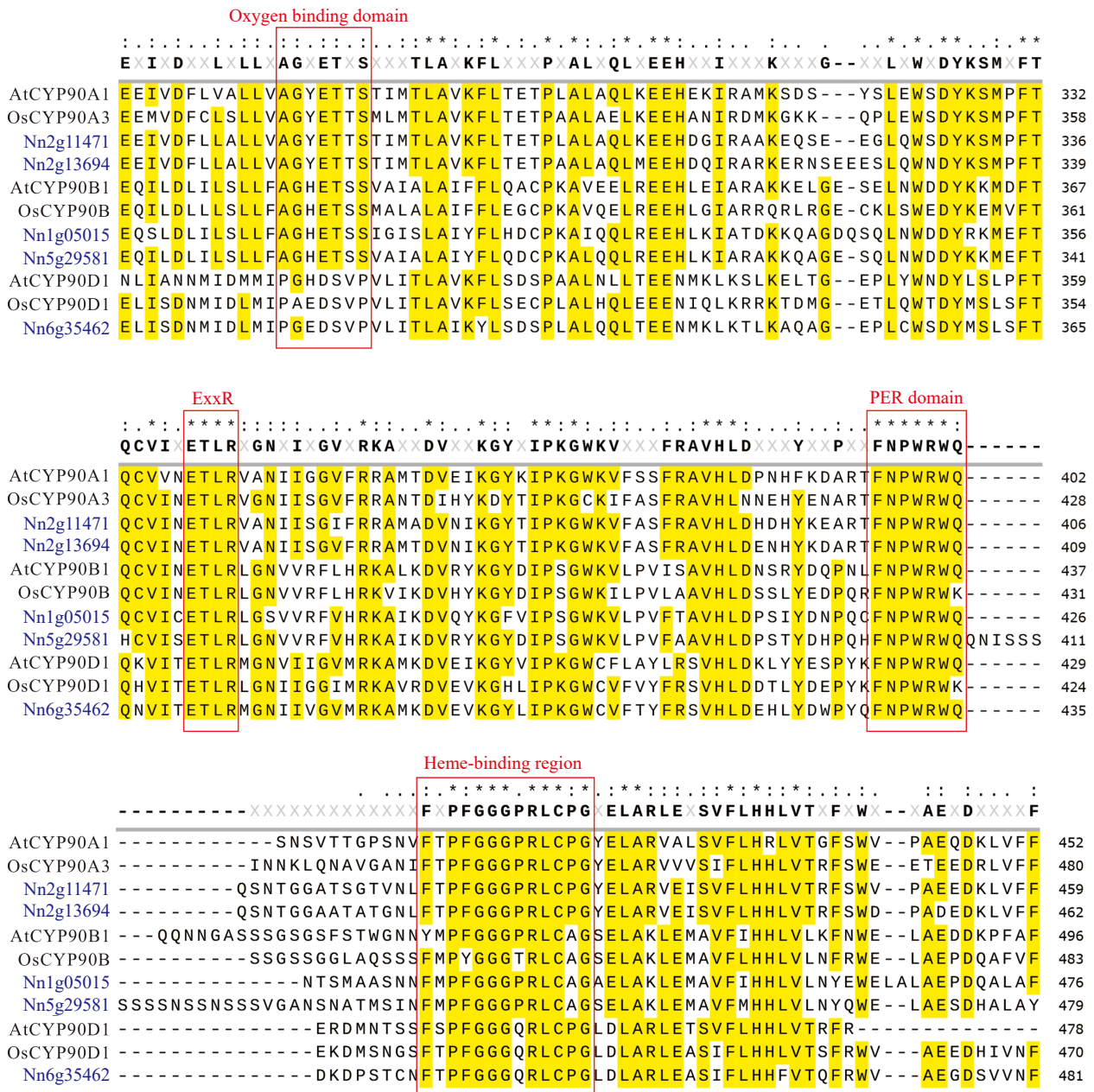


**Fig. 2** Sequence alignment of five NnCYP90 proteins with *Arabidopsis* AtCYP90A1, AtCYP90B1, AtCYP90D1, and rice OsCYP90A3, OsCYP90B, and OsCYP90D2. Conserved amino acid domains are highlighted by the red box.

of two CYP90B genes, *Nn1g05015* and *Nn5g29581*, exhibited a predominance of light response elements, such as GT1-motif, ACE, and G-box. The promoter of *Nn1g05015* featured a higher abundance of elements associated with growth and development, including an O<sub>2</sub>-site for zein metabolism regulation and a CAT-box associated with meristem expression, whereas the promoter of *Nn5g29581* contained an increased presence of hormone response elements, such as ABRE, TCA-motif (salicylic acid response), TGA-element (auxin-response), CARE, and P-box (gibberellin response). It is worth noting that, the circadian rhythm response element, circadian, was detected in the promoter of *Nn6g35462*, a unique gene within the CYP90D clade. Overall, the promoter regions of these NnCYP90s were enriched with hormone- and stress-responsive elements,

suggesting that they may play important roles in plant hormone homeostasis and adversity response.

### Transcriptomic profiling of NnCYP90s

The spatiotemporal expression profiles of *NnCYP90* genes were determined using our previously published transcriptomic data<sup>[26–28]</sup>. All five *NnCYP90* genes were exhibited expression in at least one tissue (FPKM ≥ 1). The *NnCYP90A* subfamily genes displayed expression across all tissues. Specifically, *Nn2g11471* exhibited high expression levels in leaves, whereas *Nn2g13694* showed prominent expression in flower organs, including petals, stamens, and pistils (FPKM ≥ 10). Conversely, three genes within the *NnCYP90B* and *NnCYP90D* subfamilies demonstrated specific expression in the underground tissues, notably roots, and rhizomes (Fig. 4a, b). Subsequently, it was

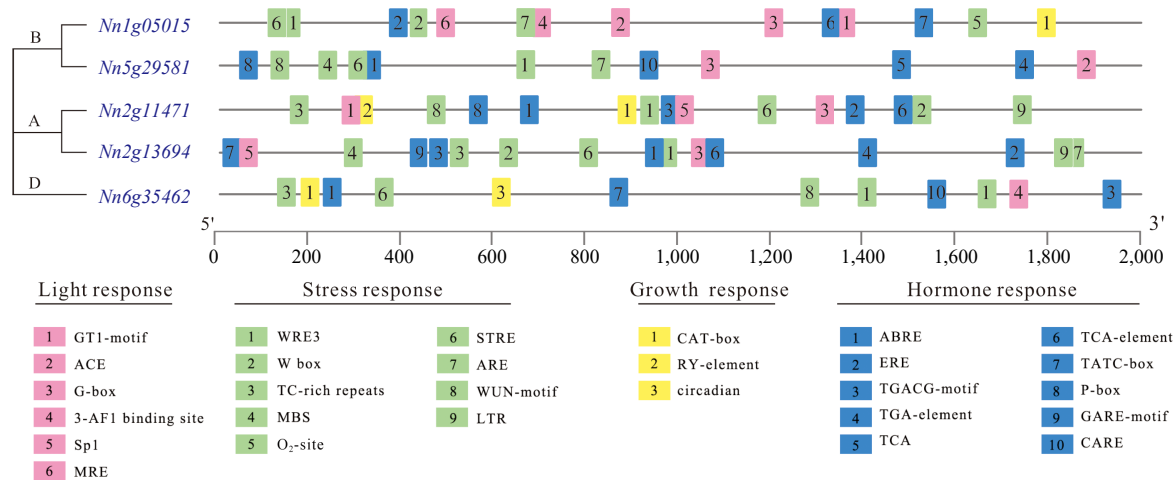


**Fig. 3** The *cis*-acting elements identified in the promoters of *NnCYP90* in lotus.

investigated whether lotus *CYP90* genes were responsive to MeJA treatment, using our MeJA transcriptomic data<sup>[27]</sup>. *NnCYP90A* and *NnCYP90D* genes exhibited responsiveness to MeJA treatment, with their expression significantly induced and peaking levels at 6 h post-treatment (Fig. 4c). Among these, *Nn2g11471* displayed the most pronounced change in expression following MeJA treatment. Conversely, *NnCYP90Bs* demonstrated insensitivity to MeJA treatment. Specifically, *Nn1g05015* was not induced by MeJA, and while *Nn5g29581* showed a slight increase in expression after 24 h post MeJA treatment (Fig. 4c). Similarly, *NnCYP90Bs* exhibited very low expression levels in embryos at all developmental stages from 9 to 24 d after pollination (DAP), whereas *NnCYP90As* and *NnCYP90D* displayed high expression levels across all embryo developmental stages. Intriguingly, two *NnCYP90A* genes exhibited opposite expression patterns. *Nn2g13694* demonstrated increased expression during embryo development, whereas the expression of *Nn2g11471* decreased significantly throughout the process (Fig. 4d).

### Validation of *NnCYP90B1* function in lotus rhizome development

*Nn5g29581*, designated as *NnCYP90B1*, was located on the flank of *cqRE1-LG2*, a major QTL associated with rhizome enlargement<sup>[5]</sup>, and was prominently expressed in underground tissues (Fig. 4). Therefore, it was speculated that it might be involved in lotus rhizome enlargement. This speculation was substantiated through the analysis of its expression profiles and by conducting transformation experiments in potato plants.

Given that proteins execute specific biological functions within distinct subcellular organelles, an *NnCYP90B1*-GFP fusion protein was created and transiently expressed in *N. benthamiana*. Subcellular localization assays revealed predominant GFP signal within the ER, aligning with predictions of *NnCYP90B* as an ER-localized protein and consistent with typical localization patterns of CYP proteins (Fig. 5a).

Further examination involved assessing the spatial and temporal expression profiles of *NnCYP90B1* across various tissues of the temperate lotus 'ZO' and the tropical lotus 'DH' were assessed using RT-qPCR analysis. The results unveiled a congruent expression pattern for *NnCYP90B1* in both lotus ecotypes, with significantly heightened expression levels in

roots and comparatively lower levels in aboveground tissues. Remarkably, petioles and pedicels exhibited the lowest expression levels, while rhizomes displayed significantly higher expression in 'ZO' compared to 'DH' (Fig. 5b). Meanwhile, comparing *NnCYP90B1* transcript levels across two stages of 'ZO', the stolon stage and swelling stage, revealed consistent dominance of expression in underground tissues. Notably, the expression of *NnCYP90B1* was significantly up-regulated during the swelling period compared with the stolon stage, except for the pedicels (Fig. 5c). These findings suggest a potential role for *NnCYP90B1* in influencing rhizome development and serving as a pivotal factor in lotus rhizome enlargement.

To further investigate the hypothesis that *NnCYP90B1* regulates the initiation of rhizome formation, two stable *Solanum tuberosum* lines overexpressing *NnCYP90B1* were obtained and confirmed *via* PCR detection (Fig. 6a). Compared to the control E3 lines, the overexpressing lines exhibited significantly earlier tuberization. On average, E3 lines produced tubers 94 d after planting. In contrast, overexpressing lines #30 and #51 initiated tuberization 13 and 17 d earlier, respectively, than the control lines. Additionally, the number and weight of tubers per plant significantly increased in the transgenic lines. The average number of tubers per plant in the transgenic lines increased by 1~2 times compared to the E3 lines. Moreover, the total weight per plant increased by more than fivefold (Table 3; Fig. 6b, c). To elucidate the impact of *NnCYP90B1* on the potato tuberization pathway, the expression of *StSP6A* and *StSP5G*, two known key genes in the tuberization pathway, was assessed. In the overexpressed plants, an increasing trend was observed in the expression levels of *StSP6A*, the tuberization-promoting gene (Fig. 6d). However, there was no detectable expression of *StSP5G*, the tuberization inhibitor, in either the transgenic lines or the control. These results suggested that the promotion of tuberization by *NnCYP90B1* in potatoes may rely on its regulatory influence on the pivotal tuber-forming gene.

### Discussion

Brassinosteroids recognized as the sixth major class of phytohormones, play an important role in the overall growth and development of plants<sup>[35]</sup>. Among the enzymes responsible for catalyzing structural modifications across the sterol skeleton, CYP450 members, particularly CYP90, hold significant

*NnCYP90B1* is involved in lotus rhizome enlargement

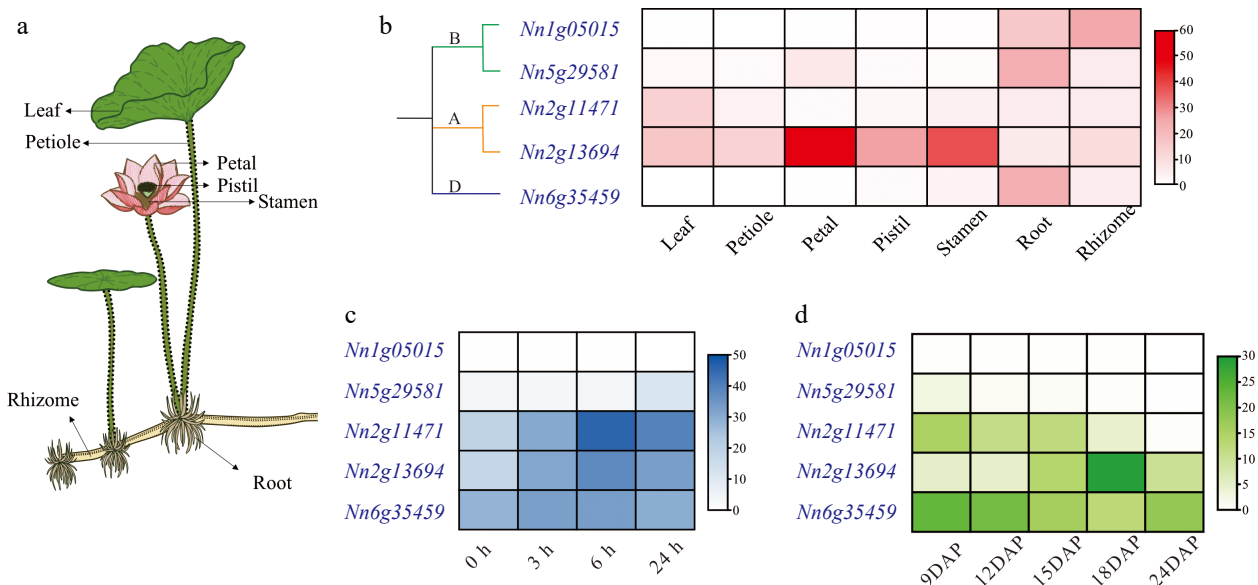


**Fig. 4** Expression patterns of *NnCYP90*s. (a) Schematic depiction of seven tissues from lotus. (b) Spatial expression profiles of *NnCYP90* in seven tissues. (c) Temporal expression profiles of *NnCYP90* in leaves treated with 100  $\mu$ M MeJA over a time course (0, 3, 6, 24 h). (d) Temporal expression profiles of *NnCYP90* in embryos at different development DAP.

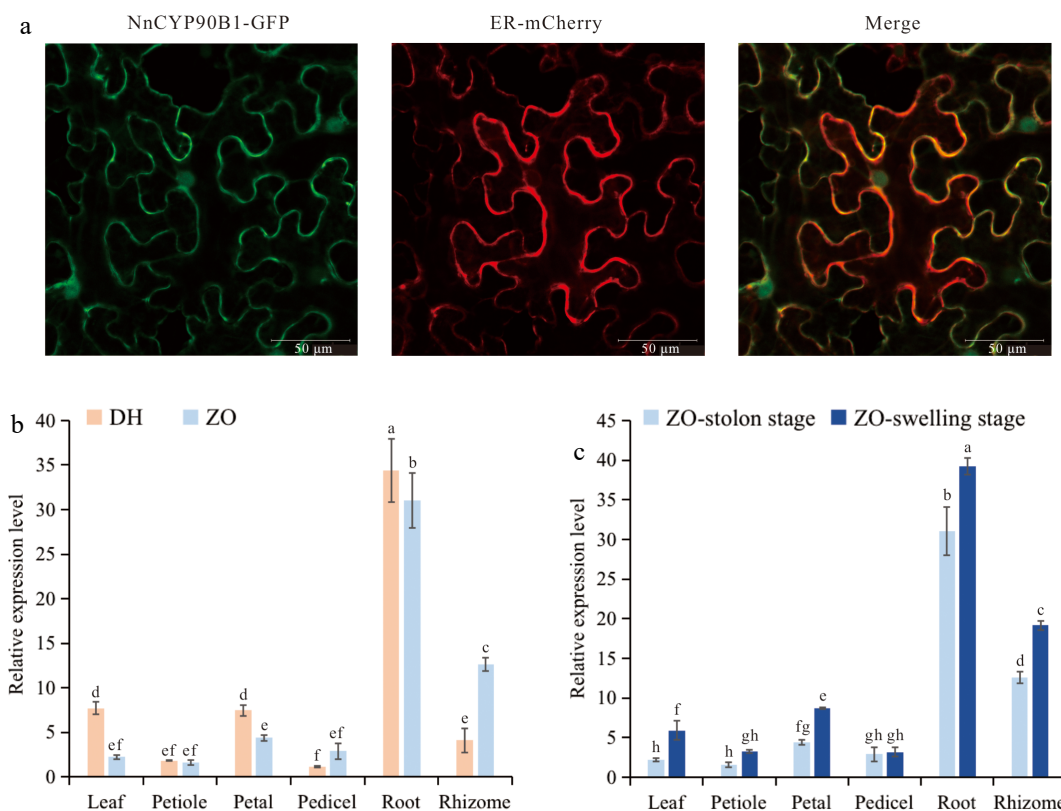


**Fig. 5** Expression patterns of *NnCYP90B1*. (a) Subcellular localization of *NnCYP90B1* in *Nicotiana benthamiana*. Bar = 50  $\mu$ m. (b) Relative expression levels of *NnCYP90B1* measured by RT-qPCR in various tissues of temperate lotus 'ZO' and tropical lotus 'DH'. (c) Relative expression levels of *NnCYP90B1* in 'ZO' different tissues before and after rhizome enlargement. Values are presented as means  $\pm$  SD from three biological replicates. Letters above each column represent significant differences based on one-way analysis of variance (ANOVA) followed by Tukey's test ( $p < 0.05$ ).

importance<sup>[17]</sup>. In this study, five *CYP90* genes distributed on four chromosomes were identified in *N. nucifera*, designated as *Nn1g05015*, *Nn2g11471*, *Nn2g13694*, *Nn5g29581*, and *Nn6g35462*, respectively. Through phylogenetic analysis, *NnCYP90*

was further classified into three subfamilies: A, B, and D. Comparison with the *NnCYP450* analysis of Nelson & Schuler revealed two members each in the *NnCYP90A* and *NnCYP90B* subfamilies, while *NnCYP90D* had one member<sup>[36]</sup>. Notably, the

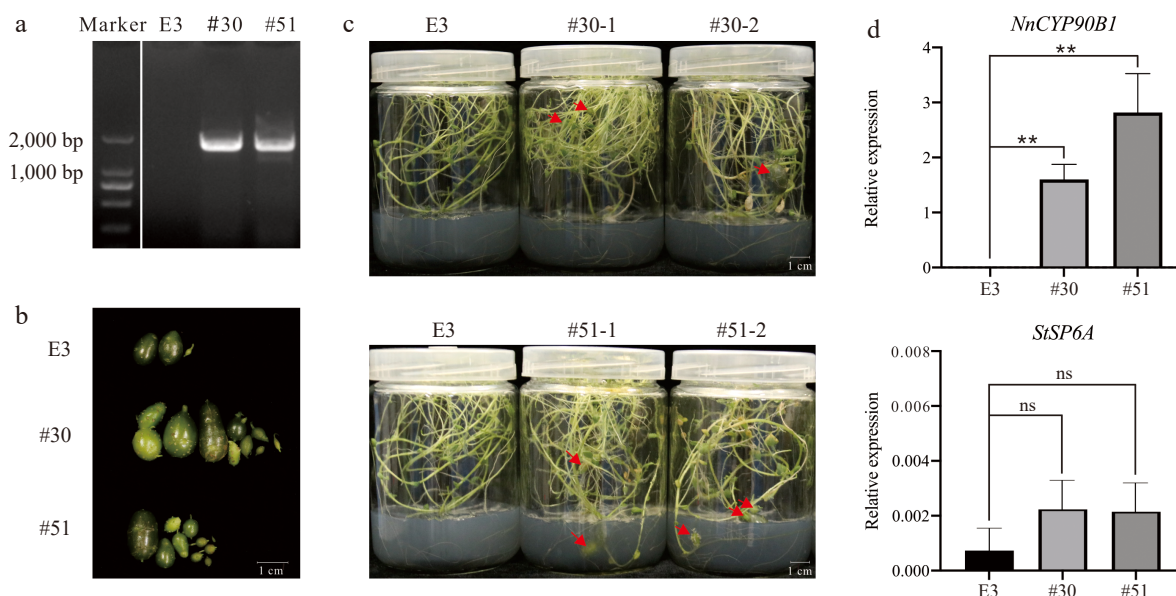


**Fig. 6** Functional validation of heterologous transformation of *NnCYP90B1* in potato. (a) PCR analysis of *NnCYP90B1* in E3 and transgenic lines #30 and #51. (b), (c) Tubers of control line E3 and transgenic plants #30 and #51 cultured in medium for 3 months. Scale bar = 1 cm. (d) RT-qPCR analysis of *NnCYP90B1* and *StSP6A* in E3 and transgenic lines #30 and #51. Values are presented as means  $\pm$  SD from three biological replicates. Asterisks indicate significant differences between transgenic lines and E3 by Tukey's test (\*\*,  $p < 0.01$ ). ns, not significant.

**Table 3.** Phenotypic statistics of over-expressed *NnCYP90B* potato lines.

| Line | Tuberization times (days after planting) | Total numbers (/plant) | Total weight (g/plant) |
|------|--|------------------------|------------------------|
| E3   | 94                                       | 1.5                    | 0.125                  |
| #30  | 81                                       | 5.0                    | 0.570                  |
| #51  | 77                                       | 3.0                    | 1.105                  |

NnCYP90C was not definitively identified in this study due to stringent identification criteria, wherein sequences lacking complete conserved structural domains were excluded (Fig. 1a). Additionally, the CYP90C and CYP90D subfamily, known for functional redundancy<sup>[37]</sup>, were found to cluster together in the evolutionary tree, with TcCYP90C1 unexpectedly positioned close to the CYP90D genes (Fig. 1a).

CYP450 family proteins share a common overall folding form in secondary structure. The sulfur atom of the completely conserved cysteine coordinates with heme iron to form a heme reaction center, facilitating the transfer of electrons from the NADPH donor to the oxygen acceptor<sup>[38,39]</sup>. Analysis indicated that the motifs of NnCYP90 are conserved, featuring a heme-binding region that includes a conserved cysteine (Fig. 1b; Fig. 2). Furthermore, the sequences of ETLR, located in the helix K region, and PWRW, located in the PER structural domain, were identical across NnCYP90 proteins, suggesting a specific set of amino acid patterns conserved in the CYP90 family (Fig. 2). Notably, the three subfamilies of NnCYP90 exhibit characteristic amino acid variations, such as proline-to-alanine substitution in the PER module of the NnCYP90A family, substitutions at two amino acid positions in the heme-binding region of the NnCYP90B family, and the absence of an oxygen-binding domain in NnCYP90D (Fig. 2). Collectively, these findings suggest that while NnCYP90 proteins maintain conserved CYP450 functions, they also possess different enzymatic functions attributable to their distinct sequence features.

The rhizome serves as a crucial storage organ for the lotus and also facilitates vegetative propagation. Its enlargement is an adaptive strategy for enduring the cold winter. Despite its importance, detailed studies on the molecular mechanisms involved are lacking. Previous studies suggest a complex process of growth regulation, with hormones such as GA and ABA playing pivotal roles that vary with the photoperiod. It has been demonstrated that the external application of GA can promote rhizome elongation. However, the application of GA inhibitors can stimulate rhizome enlargement under LD conditions. ABA and light may be transduced through secondary messenger  $Ca_2^+$ , and play important roles in lotus rhizome enlargement<sup>[9]</sup>. In addition to GA and ABA, BR signaling has been identified as a promoter of growth during both vegetative and reproductive development in lotus. External application of 28-epihomobrassinolide induces growth-promoting phenotypes, including longer scapes, thicker leaves, and prolonged flowering<sup>[40]</sup>. However, the effects of BR on lotus rhizome development remain largely unexplored. Understanding and manipulating the BR signaling pathway holds significant agricultural promise for improving lotus rhizome yield and quality. Here, it was noted that the gene *NnCYP90B1* (*Nn5g29581*) was located on the flank of *cqREI-LG2* and conservatively clustered with CYP90B of six other species. CYP90B is a key rate-limiting enzyme in the BR biosynthetic pathway, catalyzing the C22 $\alpha$ -hydroxylation reaction of the sterol skeleton<sup>[33]</sup>. In *Arabidopsis*, *AtCYP90B1* is expressed in stems, leaves, shoots, and roots, with higher expression observed in apical shoots, which contain actively developing tissues<sup>[41]</sup>. In contrast, the expression profile of *NnCYP90B1* in *N. nucifera* differs significantly, showing high expression in underground tissues and a strong correlation with rhizome enlargement (Fig. 4; Fig. 5). Investigating whether NnCYP90B1 plays a role in rhizome enlargement will be intriguing.

Potato is an ideal heterologous transformation material for studying tuber enlargement mechanisms, which have been

*NnCYP90B1* is involved in lotus rhizome enlargement

deeply investigated in their own right. Tuber enlargement in potatoes is a complex physiological process influenced by a sophisticated interplay of plant hormones, genetic factors, and environmental conditions. Numerous studies have demonstrated the significant impact of various hormones on tuber formation. High levels of GA promote stolon sprouting but are detrimental to tuber formation, whereas ABA has a positive effect on tuber induction. Similarly, JA and BR also contribute to tuber formation<sup>[42]</sup>. During potato tuber induction, three key regulatory proteins, StCDF1, StSP6A, and StBEL5, play critical roles. Of these, StSP6A is a crucial component of tuberigen, forming a tuberigen activation complex (TAC) with St14-3-3 and StFDL1, essential for initiating tuber development<sup>[43]</sup>. The heterologous transformation of *NnCYP90B1* into potatoes resulted in earlier tuber setting and an increased number of tubers (Fig. 6), consistent with the action of *NnBEL6*, which regulates lotus rhizome enlargement<sup>[5]</sup>. Simultaneously, efforts were made to elucidate the molecular mechanisms underlying the involvement of *NnCYP90B* in rhizome enlargement. Analysis of *StSP6A* expression levels revealed an upward trend in overexpressed lines, although no significant differences compared to the control were observed. It was predicted that there is no direct regulatory relationship between *NnCYP90B1* and *StSP6A*. In conclusion, *NnCYP90B1* acts as a positive regulator in promoting rhizome enlargement. The regulation of rhizome enlargement is a complex developmental process, further systematic studies are warranted to fully elucidate the mechanism of rhizome enlargement. The discovery of the *NnCYP90B1* gene function offers a new perspective for such investigations.

## Author contributions

The authors confirm contribution to the paper as follows: study conception and design: Yang M; draft manuscript preparation: Zhang M. Manuscript revision: Song H, Deng X. All authors reviewed the results and approved the final version of the manuscript.

## Data availability

The datasets generated during and/or analyzed during the current study are available from the corresponding author on reasonable request.

## Acknowledgments

This project was supported by funds received from the Hubei Province Supporting High Quality Development Fund Project for Seed Industry (Grant no. HBZY2023B004-1) and the National Natural Science Foundation of China (Grant Nos 32070336; 32370428)

## Conflict of interest

The authors declare that they have no conflict of interest.

## Dates

Received 16 March 2024; Revised 7 August 2024; Accepted 13 August 2024; Published online 2 December 2024

## References

- Lin Z, Zhang C, Cao D, Damaris RN, Yang P. 2019. The latest studies on lotus (*Nelumbo nucifera*)—an emerging horticultural model plant. *International Journal of Molecular Sciences* 20:3680
- Cao D, Damaris RN, Zhang Y, Liu M, Li M, et al. 2019. Proteomic analysis showing the signaling pathways involved in the rhizome enlargement process in *Nelumbo nucifera*. *BMC Genomics* 20:766
- Cheng L, Li S, Yin J, Li L, Chen X. 2013. Genome-wide analysis of differentially expressed genes relevant to rhizome formation in lotus root (*Nelumbo nucifera* Gaertn.). *PLoS ONE* 8:e67116
- Yang M, Zhu L, Pan C, Xu L, Liu Y, et al. 2015. Transcriptomic analysis of the regulation of rhizome formation in temperate and tropical lotus (*Nelumbo nucifera*). *Scientific Reports* 5:13059
- Liu Y, Song H, Zhang M, Yang D, Deng X, et al. 2022. Identification of QTLs and a putative candidate gene involved in rhizome enlargement of Asian lotus (*Nelumbo nucifera*). *Plant Molecular Biology* 110:23–36
- Masuda JI, Ozaki Y, Okubo H. 2007. Rhizome transition to storage organ is under phytochrome control in lotus (*Nelumbo nucifera*). *Planta* 226:909–15
- Masuda J, Yoshimizu S, Ozaki Y, Okubo H. 2007. Rhythmic response of rhizome growth to light-break in lotus (*Nelumbo nucifera*). *Journal of the Faculty of Agriculture, Kyushu University* 52:35–38
- Masuda J, Ozaki Y, Miyajima I, Okubo H. 2010. Ethylene is not involved in rhizome transition to storage organ in lotus (*Nelumbo nucifera*). *Journal of the Faculty of Agriculture, Kyushu University* 55:231–32
- Masuda JI, Ozaki Y, Okubo H. 2012. Regulation in rhizome transition to storage organ in lotus (*Nelumbo nucifera* Gaertn.) with exogenous gibberellin, gibberellin biosynthesis inhibitors or abscisic acid. *Journal of the Japanese Society for Horticultural Science* 81:67–71
- Mitchell JW, Mandava N, Worley JF, Plimmer JR, Smith MV. 1970. Brassins—a new family of plant hormones from rape pollen. *Nature* 225:1065–66
- Nolan TM, Vukašinić N, Liu D, Russinova E, Yin Y. 2020. Brassinosteroids: multidimensional regulators of plant growth, development, and stress responses. *The Plant Cell* 32:295–318
- Ramraj VM, Vyas BN, Godrej NB, Mistry KB, Swami BN, et al. 1997. Effects of 28-homobrassinolide on yields of wheat, rice, groundnut, mustard, potato and cotton. *The Journal of Agricultural Science* 128:405–13
- Guo C, Shen Y, Li M, Chen Y, Xu X, et al. 2022. Principal component analysis to assess the changes of yield and quality of two *Pinellia ternata* cultivars after Brassinolide treatments. *Journal of Plant Growth Regulation* 41:2185–97
- Tang X, Qu Z, Zhang H, Wei Q, Zhang L, et al. 2018. Effect of physiology and yield by spraying EBR during potato tuber formation stage. *Journal of Nuclear Agricultural Sciences* 32:1855–63
- Doležalová J, Koudela M, Sus J, Ptáček V. 2016. Effects of synthetic brassinolide on the yield of onion grown at two irrigation levels. *Scientia Horticulturae* 202:125–32
- Bajguz A, Piotrowska-Niczyporuk A. 2023. Biosynthetic pathways of hormones in plants. *Metabolites* 13:884
- Ghosh S. 2017. Triterpene structural diversification by plant cytochrome P450 enzymes. *Frontiers in Plant Science* 8:1886
- Szekeres M, Nemeth K, Koncz-Kalman Z, Mathur J, Kauschmann A, et al. 1996. Brassinosteroids rescue the deficiency of CYP90, a cytochrome P450, controlling cell elongation and de-etiolation in *Arabidopsis*. *Cell* 85:171–82
- Choe S, Dilkes BP, Fujioka S, Takatsuto S, Sakurai A, et al. 1998. The *dwf4* gene of *Arabidopsis* encodes a cytochrome P450 that mediates multiple 22 $\alpha$ -hydroxylation steps in brassinosteroid biosynthesis. *The Plant Cell* 10:231–43

20. Kim GT, Fujioka S, Kozuka T, Tax FE, Takatsuto S, et al. 2005. CYP90C1 and CYP90D1 are involved in different steps in the brassinosteroid biosynthesis pathway in *Arabidopsis thaliana*. *The Plant Journal* 41:710–72
21. Sakamoto T, Morinaka Y, Ohnishi T, Sunohara H, Fujioka S, et al. 2006. Erect leaves caused by brassinosteroid deficiency increase biomass production and grain yield in rice. *Nature Biotechnology* 24:105–09
22. Bishop GJ, Harrison K, Jones JD. 1996. The tomato *Dwarf* gene isolated by heterologous transposon tagging encodes the first member of a new cytochrome P450 family. *The Plant Cell* 8:959–69
23. Koka CV, Cerny RE, Gardner RG, Noguchi T, Fujioka S, et al. 2000. A putative role for the tomato genes *DUMPY* and *CURL-3* in brassinosteroid biosynthesis and response. *Plant Physiology* 122:85–98
24. Chen C, Chen H, Zhang Y, Thomas HR, Frank MH, et al. 2020. TBtools: an integrative Toolkit developed for interactive analyses of big biological data. *Molecular Plant* 13:1194–202
25. Chou KC, Shen HB. 2008. Cell-PLoc: a package of Web servers for predicting subcellular localization of proteins in various organisms. *Nature Protocols* 3:153–62
26. Shi T, Rahmani RS, Gugger PF, Wang M, Li H, et al. 2020. Distinct expression and methylation patterns for genes with different fates following a single whole-genome duplication in flowering plants. *Molecular Biology and Evolution* 37:2394–413
27. Li J, Xiong Y, Li Y, Ye S, Yin Q, et al. 2019. Comprehensive analysis and functional studies of WRKY transcription factors in *Nelumbo nucifera*. *International Journal of Molecular Sciences* 20:5006
28. Sun H, Song H, Deng X, Liu J, Yang D, et al. 2022. Transcriptome-wide characterization of alkaloids and chlorophyll biosynthesis in lotus plumule. *Frontiers in Plant Science* 13:885503
29. Zhou T, Song B, Liu T, Shen Y, Dong L, et al. 2019. Phytochrome F plays critical roles in potato photoperiodic tuberization. *The Plant Journal* 98:42–54
30. Navarro C, Abelenda JA, Cruz-Oró E, Cuellar CA, Tamaki S, et al. 2011. Control of flowering and storage organ formation in potato by FLOWERING LOCUS T. *Nature* 478:119–22
31. Zhan H, Lu M, Luo Q, Tan F, Zhao Z, et al. 2022. *OsCPD1* and *OsCPD2* are functional brassinosteroid biosynthesis genes in rice. *Plant Science* 325:111482
32. Wang M, Xu X, Zhang X, Sun S, Wu C, et al. 2015. Functional analysis of *GmCPDs* and investigation of their roles in flowering. *PLoS ONE* 10:e0118476
33. Fujita S, Ohnishi T, Watanabe B, Yokota T, Takatsuto S, et al. 2006. *Arabidopsis* CYP90B1 catalyses the early C-22 hydroxylation of C<sub>27</sub>, C<sub>28</sub> and C<sub>29</sub> sterols. *The Plant Journal* 45:765–74
34. Marand AP, Eveland AL, Kaufmann K, Springer NM. 2023. *cis*-regulatory elements in plant development, adaptation, and evolution. *Annual Review of Plant Biology* 74:111–37
35. Sun Y, Fan X, Cao D, Tang W, He K, et al. 2010. Integration of brassinosteroid signal transduction with the transcription network for plant growth regulation in *Arabidopsis*. *Developmental Cell* 19:765–77
36. Nelson DR, Schuler MA. 2013. Cytochrome P450 genes from the sacred lotus genome. *Tropical Plant Biology* 6:138–51
37. Ohnishi T, Szatmari AM, Watanabe B, Fujita S, Bancos S, et al. 2006. C-23 hydroxylation by *Arabidopsis* CYP90C1 and CYP90D1 reveals a novel shortcut in brassinosteroid biosynthesis. *The Plant Cell* 18:3275–88
38. Šrejšber M, Navrátilová V, Paloncýová M, Bazgier V, Berka K, et al. 2018. Membrane-attached mammalian cytochromes P450: an overview of the membrane's effects on structure, drug binding, and interactions with redox partners. *Journal of Inorganic Biochemistry* 183:117–36
39. Syed K, Mashele SS. 2014. Comparative analysis of P450 signature motifs EXXR and CXG in the large and diverse kingdom of fungi: identification of evolutionarily conserved amino acid patterns characteristic of P450 family. *PLoS ONE* 9:e95616
40. Sheng J, Li X, Zhang D. 2022. Gibberellins, brassinolide, and ethylene signaling were involved in flower differentiation and development in *Nelumbo nucifera*. *Horticultural Plant Journal* 8:243–50
41. Shimada Y, Goda H, Nakamura A, Takatsuto S, Fujioka S, et al. 2003. Organ-specific expression of brassinosteroid-biosynthetic genes and distribution of endogenous brassinosteroids in *Arabidopsis*. *Plant Physiology* 131:287–97
42. Saidi A, Hajibarat Z. 2021. Phytohormones: plant switchers in developmental and growth stages in potato. *Journal of Genetic Engineering and Biotechnology* 19:89
43. Teo CJ, Takahashi K, Shimizu K, Shimamoto K, Taoka KI. 2017. Potato tuber induction is regulated by interactions between components of a tuberigen complex. *Plant and Cell Physiology* 58:365–74



Copyright: © 2024 by the author(s). Published by Maximum Academic Press, Fayetteville, GA. This article is an open access article distributed under Creative Commons Attribution License (CC BY 4.0), visit <https://creativecommons.org/licenses/by/4.0/>.